Clim. Past Discuss., 6, 1337–1350, 2010
www.clim-past-discuss.net/6/1337/2010/
doi:10.5194/cpd-6-1337-2010

Climate
of the Past
Discussions

# Uncertainty of the $CO_2$ threshold for melting a hard Snowball Earth

**Y. Hu and J. Yang**

Dept. of Atmospheric and Oceanic Sciences, School of Physics, Peking University,
Beijing 100871, China

Received: 20 June 2010 – Accepted: 1 July 2010 – Published: 12 July 2010

Correspondence to: Y. Hu (yyhu@pku.edu.cn)

Published by Copernicus Publications on behalf of the European Geosciences Union.

## Abstract

One of the critical issues of the Snowball Earth hypothesis is how high level of $CO_2$ is required for triggering the deglaciation. Using Community Atmospheric Model version 3 (CAM3), we study the problem for the $CO_2$ threshold. Our simulations show large differences from previous results (Pierrehumbert, 2004, 2005). At 0.2 bars of $CO_2$, the January maximum near-surface temperature is about 268 K, about 13 K higher than that in Pierrehumbert (2004, 2005), but lower than the value of 270 K for 0.1 bar of $CO_2$ in Le Hir et al. (2007). It is found that the diversity of simulation results is mainly due to model sensitivity of greenhouse effect and longwave cloud forcing to increasing $CO_2$. At 0.2 bar of $CO_2$, CAM3 yields 117 $Wm^{-2}$ of clear-sky greenhouse effect and 32 $Wm^{-2}$ of longwave cloud forcing, versus only about 77 $Wm^{-2}$ and 10.5 $Wm^{-2}$ in Pierrehumbert (2004, 2005), respectively. CAM3 has comparable clear-sky greenhouse effect to that in Le Hir et al. (2007), but lower longwave cloud forcing. CAM3 also produces much stronger Hadley cells than in Pierrehumbert (2005).

## 1 Introduction

The Snowball Earth hypothesis is probably one of the most intriguing and fundamental problems in paleoclimate research in the past 10 years and received intensive debate (Kirschvink, 1992; Hoffman et al., 1998; Hoffman and Schrag, 2002). One of the important issues in Snowball Earth studies is the threshold of $CO_2$ concentration to rescue Earth from global glaciations (Pierrehumbert, 2004, 2005). According to the Snowball Earth hypothesis, the Snowball Earth was deglaciated by strong greenhouse effect of high-level $CO_2$, which was accumulated due to volcanic eruptions over time scale of tens of millions of years when weathering reactions between $CO_2$ and surface rocks were cut off by snow-ice coverage.

The $CO_2$ threshold was estimated by simulation studies with both energy balance models (EBMs) and general circulation models (GCMs). EBMs yielded a wide range of values (Caldeira and Kasting, 1992; Hyde et al., 2000; Tajika, 2003). As commented by Pierrehumbert (2005), these different values would converge to about 0.2 ~ 0.3 bars of $CO_2$ as consistent conditions are considered. GCMs have more realistic dynamical and physical processes compared with EBMs and would provide more reliable results. However, GCM simulations also yielded different $CO_2$ thresholds. Using the fast oceanic atmospheric model (FOAM), Pierrehumbert (2004, 2005) found that even for 0.2 bars of $CO_2$ the annual-mean surface temperature at the equator is 30 K short of the melting point, suggesting that increasing $CO_2$ alone would be very difficult to melt the hard Snowball Earth, and that other mechanisms or feedback processes are needed. Indeed, Abbot and Pierrehumbert (2010) showed that the required $CO_2$ level can be much lower (e.g., 0.01 ~ 0.1 bar) if there forms a volcanic dust layer over the tropical surface. The dust layer largely lowers the tropical surface albedo, so that deglaciation can be triggered at lower $CO_2$ levels. Using a different atmospheric GCM (LMDz), Le Hir et al. (2007) reported that the hard Snowball Earth can be melted at 0.45 bars of $CO_2$. They showed the major difference between LMDz and FOAM is that LMDz produces much larger longwave cloud forcing (Hereafter, Pierrehumbert (2004, 2005) and Le Hir et al. (2007) are also referred as FOAM and LMDz, respectively). The diversity of GCM simulations suggests that the $CO_2$ threshold is model dependent, as pointed out by Pierrehumbert (2005).

In the present study, we report different simulation results of the $CO_2$ threshold from previous studies. We also show that the differences are not only reflected in radiation, thermodynamics and cloud physics, but also in atmospheric dynamics, such as the Hadley circulation.

## 2 Model and experiments

The model used here is the CAM3 developed by the National Center for Atmospheric Research (Collins et al., 2004). It has a horizontal resolution of approximately 2.8° × 2.8° in latitude and longitude and 26 vertical levels from the surface to (approximately) 2.0 hPa. CAM3 includes a thermodynamic sea-ice model, similar to the Community Sea Ice Model (Briegleb et al., 2004), with which snow depth, surface temperature, surface albedo, and energy fluxes between ice and overlying atmosphere can be predicted, while ice thickness and ice fractional coverage are both prescribed by fixing surface temperature over ice below the model freezing point: −1.8 °C (271.35 K).

To simulate a hard snowball earth, we prescribe an ocean covered by fixed sea ice with thickness of 20 m. An idealized rectangular supercontinent is centered at the equator as in Pierrehumbert (2004, 2005) and Poulson (2001). Sea ice is covered by a snow layer with initial depth of 1 m (liquid water equivalent). Snow depth varies with time. Solar luminosity is 94% of the present value. Eccentricity, obliquity, and rotation rate are all defined as present values. We use the same albedo values as Pierrehumbert (2005), that is, snow albedo is 0.9 and 0.6 for visible and near-infrared radiation, respectively, and the sea-ice albedo is 0.5, independent of wavelength. Various $CO_2$ levels have been set: 100, 400, 1600, 12 800 ppmv, 0.1, and 0.2 bars, same as Pierrehumbert (2004, 2005).

It is worth pointing out that the atmospheric component of FOAM used by Pierrehumbert (2004, 2005) is derived from CCSM3, i.e., one of the previous versions of CAM3. CAM3 has several significant improvements in physical parameterizations relative to CCSM3 (Collins et al., 2004), including revised cloud and precipitation parameterizations with prognostic formulations for the partitioning of cloud water between liquid and ice phases (Boville et al., 2006), updated radiation schemes for water vapor absorption in visible and infrared regions (Collins et al., 2002, 2006). As a result of these changes, CAM3 has a warmer, moister and more stable troposphere, and that major features of temperature, water vapor, cloud and precipitation in CAM3 are more consistent with observational estimates compared with that in CCSM3 (Hack et al., 2006). As shown below, these improvements cause significant differences in Snowball-Earth simulations. The results here will be compared with that in FOAM and LMDz to show model dependences.

## 3 Results

Figure 1a shows January zonal-mean air temperatures at the lowest model level ($T_{\mathrm{BOT}}$) for various $CO_2$ levels. While the bulk meridional temperature structures are similar to that in FOAM, they show much stronger hemispheric temperature contrast between summer and winter hemispheres. For 100 ppmv of $CO_2$, the maximum temperature in the summer hemisphere (Southern Hemisphere) is about 253 K, which is close to that in LMDz, but about 5 K higher than that in FOAM. The maximum temperature is located at about 45° S, which is consistent with that in LMDz, but more poleward than in FOAM. The lowest temperature of about 145 K is in the winter pole, which is about 20 K lower than in FOAM, but 10 K higher than in LMDz. As $CO_2$ level increases, $T_{\mathrm{BOT}}$ increases faster than in FOAM. At 0.2 bars of $CO_2$, the maximum $T_{\mathrm{BOT}}$ is about 268 K, about 5 K short of the freezing point. In contrast, FOAM yields a January maximum $T_{\mathrm{BOT}}$ of 255 K, and LMDz gives a value of 270 K for 0.1 bar of $CO_2$.

Figure 1b shows January maximum, global and annual mean, and annual-mean equatorial near-surface temperatures as a function of $CO_2$ levels. The temperatures show nonlinear relationship with the logarithm of $CO_2$ concentration. At low levels of $CO_2$ (100–1600 ppmv), each quadrupling of $CO_2$ causes temperatures increased by about 1.1–1.4 K, even slower than the 2 K increase in FOAM. However, temperature increases become much faster as $CO_2$ level gets higher. Especially, for $CO_2$ levels from 12 800 ppmv to 0.1 bar, the equatorial annual-mean temperature is increased by about 12 K, equivalent to 4.0 K for each doubling of $CO_2$. Temperature increase slows again as $CO_2$ increases from 0.1 to 0.2 bars. This is probably because of the sea-ice prescription that limits ice-surface temperature below $-1.8\,^{\circ}\mathrm{C}$ (271.35 K). Indeed, further increasing $CO_2$ results in $T_{\mathrm{BOT}}$ asymptotic to 271.35 K. If the equatorial annual-mean temperature of 273 K is considered as the standard for triggering the deglaciation of the Snowball Earth, as suggested by Pierrehumbert (2004, 2005), our simulations suggest that the $CO_2$ threshold would be close to 1 bar of $CO_2$ for the increasing rate of 4 K for each doubling $CO_2$. This estimated threshold is higher than that in LMDz (0.45 bars), but much more reachable for $CO_2$ accumulation than that in FOAM.

What cause different model sensitivities of near-surface temperatures to increasing $CO_2$? This can be demonstrated by evaluating the clear-sky greenhouse effect and longwave cloud forcing, by following Pierrehumbert (2004, 2005). Figure 2a shows the clear-sky greenhouse effect in January for various levels of $CO_2$. At 100 ppmv of $CO_2$, the maximum clear-sky greenhouse effect is about 50 $\mathrm{W m^{-2}}$. It is close to that in LMDz, but about 20 $\mathrm{W m^{-2}}$ higher than in FOAM. As $CO_2$ increases to 0.1 bar, the maximum clear-sky greenhouse effect is up to 110 $\mathrm{W m^{-2}}$. It is about 5 and 45 $\mathrm{W m^{-2}}$ higher than that in LMDz and FOAM, respectively. The stronger clear-sky greenhouse effect is presumably due to the improvement in radiation scheme for water vapor in CAM3, which increases the near-infrared absorption by water vapor and leads to a warmer and moister atmosphere (Collins et al., 2006). Increasing water vapor in the atmosphere consequently causes a stronger greenhouse effect. The location of the maximum clear-sky greenhouse effect also shows different meridional shifts from that in FOAM as $CO_2$ increases. It shifts equatorward from about 45° S for 100 ppmv $CO_2$ to about 30° S for 0.2 bar of $CO_2$. Such a shift is consistent with that in LMDz, but opposite to that in FOAM.

For the cold snowball earth condition, clouds exist mainly in the form of ice particles and thus have greenhouse effect, as pointed out by Pierrehumbert (2004, 2005). In FOAM, longwave cloud forcing is about 6 $\mathrm{W m^{-2}}$ for 100 ppmv of $CO_2$ and about 10.5 $\mathrm{W m^{-2}}$ for 0.2 bar of $CO_2$. In contrast, CAM3 has a much stronger longwave cloud forcing. Figure 2b shows longwave cloud forcing in January for various levels of $CO_2$. Unlike that in FOAM, the maximum longwave cloud forcing is located in middle latitudes of the summer hemisphere for low levels of $CO_2$, rather than around 12° S, and the maximum cloud forcing at middle latitudes decreases with $CO_2$ levels. We will address this phenomenon later.

Around 12° S, longwave cloud forcing increases with $CO_2$ levels. This is because increasing $CO_2$ warms the tropical surface, which leads to stronger upward motion associated with the Hadley circulation. Thus, more water vapor is transported into the atmosphere, causing more ice clouds and stronger greenhouse effect. For 100 ppmv, the maximum cloud forcing is about 26 $Wm^{-2}$, about 20 $Wm^{-2}$ higher than in FOAM. For 0.2 bars of $CO_2$, the cloud forcing is up to 32 $Wm^{-2}$, about 21.5 $Wm^{-2}$ higher than the FOAM value. The longwave cloud forcing in CAM3 is higher than in FOAM. However, it is lower than that in LMDz. For 330 ppmv of $CO_2$, the maximum cloud forcing is 50 $Wm^{-2}$ in LMDz, which is twice larger than the 23 $Wm^{-2}$ for 400 ppmv of $CO_2$ in CAM3. The above results demonstrate that the higher near-surface temperatures in CAM3 than in FOAM for the same level of $CO_2$ is because both clear-sky greenhouse effect and longwave cloud forcing are much stronger in CAM3.

The decrease in maximum longwave cloud forcing at the summer-hemisphere middle latitudes can be addressed with Fig. 3. At 100 ppmv of $CO_2$, a layer with relative humidity above 80% is located between 900 and 400 hPa (Fig. 3a). According to the threshold for cloud formation in CAM3 (Collins et al., 2004), this layer is the cloud layer. Indeed, Fig. 3b shows clouds mainly exist in this layer. As $CO_2$ is up to 0.2 bars, the cloud layer is lifted to between 500 and 300 hPa. The rising of the cloud layer has two opposite effects on longwave cloud forcing. First, ice clouds at higher levels have stronger greenhouse effect since clouds emit outgoing infrared radiation at lower temperatures. Second, the rising of cloud layer causes less cloud formation because water vapor concentration decreases with altitudes (Fig. 3c), which would reduce greenhouse effect. It appears that the latter is dominant and causes the decrease in longwave cloud forcing.

Different surface albedo in these models also contributes to the difference in near-surface temperatures (Abott and Pierrehumbert, 2010). At 0.2 bars of $CO_2$, the global-mean surface albedo is 0.664 in FOAM, while it is about 0.60 in CAM3 due to more snow melting. It indicates that the surface averagely receives about 20 $Wm^{-2}$ more solar radiation in CAM3 than in FOAM. It nearly equals to the difference of longwave cloud forcing between CAM3 and FOAM.

Model dependence is not only reflected in the physics part of simulations but also in atmospheric dynamics. Figure 4a shows the meridional mass streamfunction in January for 100 ppmv of $CO_2$. The Hadley circulation has similar horizontal extent as in FOAM, but shallower in depth. A significant difference from that in FOAM is that the Hadley circulation in CAM3 is much stronger. The maximum mass streamfunction in Fig. 4a is $300 \times 10^9$ kg s$^{-1}$, versus $215 \times 10^9$ kg s$^{-1}$ in FOAM. Detailed comparison of the maximum mass streamfunction between CAM3 and FOAM is shown in Fig. 4b. In both models, the maximum mass streamfunction nonlinearly increases with the logarithm of $CO_2$ concentration, with much faster increasing in CAM3. At 0.2 bars of $CO_2$, the maximum streamfunction is about $760 \times 10^9$ kg s$^{-1}$, versus $344 \times 10^9$ kg s$^{-1}$ in FOAM. The difference is presumably due to the stronger equator-pole temperature contrast in CAM3 than in FOAM (about 90 K versus 70 K) since it is considered a major factor in determining the intensity of the Hadley circulation (Held and Hou, 1980).

## 4 Summary

We have re-examined the problem for the deglaciation of a hard Snowball Earth with CAM3. Our simulations show that CAM3 yields higher near-surface temperatures than that in FOAM at same $CO_2$ levels. The higher near-surface temperature in CAM3 is because it generates much stronger clear-sky greenhouse effect and longwave cloud forcing. At 0.2 bar of $CO_2$, the clear-sky greenhouse effect and longwave cloud forcing are 117 Wm$^{-2}$ and 32 Wm$^{-2}$, respectively, versus 77 Wm$^{-2}$ and 10.5 Wm$^{-2}$ in FOAM. The clear-sky greenhouse effect in CAM3 is close to that in LMDz. However, the longwave cloud forcing in CAM3 is much lower than in LMDz, i.e., 23 Wm$^{-2}$ versus 50 Wm$^{-2}$ for about 400 ppmv of $CO_2$. CAM3 also produces a much stronger Hadley circulation than in FOAM because of the larger equator-pole temperature contrast. All these suggest that simulations results of the Snowball Earth are model dependent and have large uncertainty. Detailed analysis and comparison of our simulations with others will be reported separately.

*Acknowledgements.* This work is supported by the National Basic Research Program of China (973 Program, 2010CB428606), the National Natural Science Foundation of China (40875042), and the Ministry of Education of China (20070001002).

## References

Abbot, D. S. and Pierrehumbert, R. T.: Mudball: Surface dust and snowball Earth deglaciation, J. Geophys. Res., 115, D03104, doi:10.1029/2009JD012007, 2010.

Boville, B. A., Rasch P. J., Hack J. J., and McCaa, J. R.: Representation of clouds and precipitation processes in the Community Atmosphere Model version 3 (CAM3), J. Climate, 19, 2162–2183, 2006.

Briegleb, B. P., Bitz, C. M., Hunke, E. C., Lipscomb, W. H., Holland, M. M., Schram, J. L., and Moritz, R. E.: Scientific description of the sea ice component in the Community Climate System Model, Version Three, Technical Note, NCAR/TN-463_STR, National Center for Atmospheric Research, Boulder, Colorado, 78 pp., 2004.

Caldeira, K. and Kasting, J. F.: Susceptibility of the early Earth to irreversible glaciation caused by carbon dioxide clouds, Nature, 359, 226–228, 1992.

Collins, W. D., Hackney, J. K., and Edwards, D. P.: An updated parameterization for infrared emission and absorption by water vapor in the National Center for Atmospheric Research Community Atmosphere Model, J. Geophys. Res., 107(D22), 4664, doi:10.1029/2001JD001365, 2002.

Collins, W. D., Lee-Taylor, J. M., Edwards, D. P., and Francis, G. L.: Effects of increased near-infrared absorption by water vapor on the climate system, J. Geophys. Res., 111, D18109, doi:10.1029/2005JD006796, 2006.

Hack, J. J., Caron, J. M., Yeager, S. G., Oleson, K. W., Holland, M. M., Truesdale, J. E., and Rasch, P. J.: Simulation of the global hydrological cycle in the CCSM Community Atmosphere Model version 3 (CAM3): Mean features, J. Climate, 19, 2199–2221, 2006.

Held, I. M. and Hou, A. Y.: Nonlinear axially symmetric circulations in a nearly inviscid atmosphere, J. Atmos. Sci., 37, 515–533, 1980.

Hoffman, P. F., Kaufman, A. J., Halverson, G. P., and Schrag, D. P.: A Neoproterozoic snowball Earth, Science, 281, 1342–1346, 1998.

Hoffman, P. F. and Schrag, D. P.: The snowball Earth hypothesis: Testing the limits of global change, Terra Nova, 14, 129–155, 2002.

Hyde, W. T., Crowley, T. J., Baum, S. K., and Peltier, W. R.: Neoproterozoic "snowball Earth" simulations with a coupled climate/ice-sheet model, Nature, 405, 425–429, 2000.

Jenkins, G. and Smith, S.: GCM simulations of snowball Earth conditions during the late Proterozoic, Geophys. Res. Lett., 26, 2263–2266, 1999.

Kirschvink, J. L.: Late Proterozoic low-latitude global glaciation: The snowball Earth, in: The Proterozoic Biosphere, edited by: Schopf, J. W. and Klein, C., Cambridge Univ. Press, New York, 51–52, 1992.

Le Hir, G., Ramstein, G., Donnadieu, Y., and Pierrehumbert, R. T.: Investigating plausible mechanisms to trigger a deglaciation from a hard snowball Earth, C. Geoscience, 339(3–4), 274–287, 2007.

Pierrehumbert, R. T.: High levels of atmospheric carbon dioxide necessary for the termination of global glaciation, Nature, 429, 646–649, 2004.

Pierrehumbert, R. T.: Climate dynamics of a hard snowball Earth, J. Geophys. Res., 110, D01111, doi:10.1029/2004JD005162, 2005.

Poulsen, C., Pierrehumbert, R. T., and Jacob, R.: Impact of ocean dynamics on the simulation of the Neoproterozoic "snowball Earth", Geophys. Res. Lett., 28, 1575–1578, 2001.

Rasch, P. J., Boville, B. A., Hack, J. J., Mccaa, J. R. , Williamson, D. L., Kiehl, J. T., and Briegleb, B. P.: Description of the NCAR Community Atmosphere Model: CAM3.0, Technical Note, NCAR/TN-464_STR, National Center for Atmospheric Research, Boulder, Colorado, 226 pp., available online: http://www.ccsm.ucar.edu/models/atm-cam, 2004.

Tajika, E.: Faint young Sun and the carbon cycle: Implication for the Proterozoic global glaciations, Earth Planet. Sc. Lett., 214, 443–453, 2003.

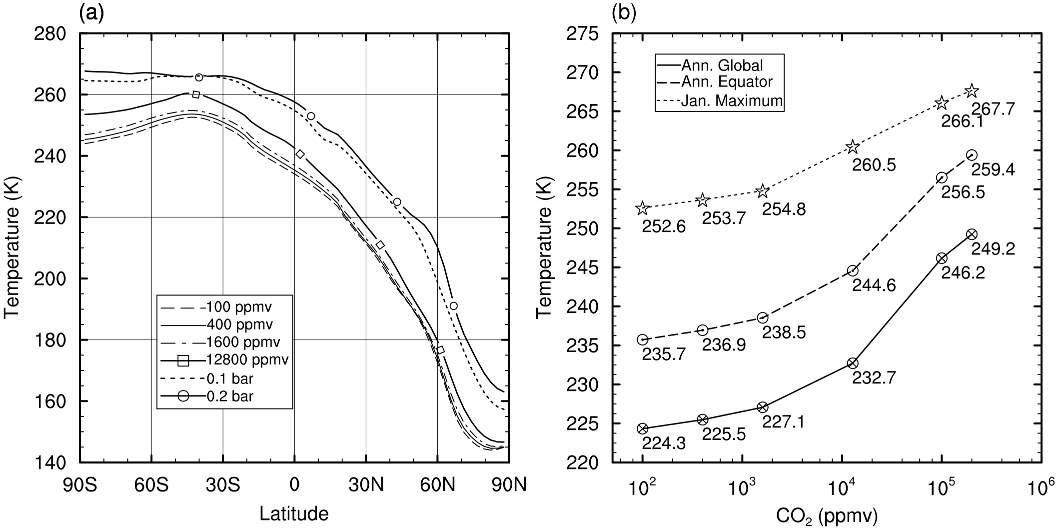

**Fig. 1.** **(a)** January zonal-mean air temperatures at the bottom model level for various $CO_2$ levels. Only sea-ice grid points are used in computing zonal-mean temperatures. **(b)** January zonal-mean maximum, equatorial annual-mean, and global annual-mean near-surface temperatures as a function of $CO_2$ levels.

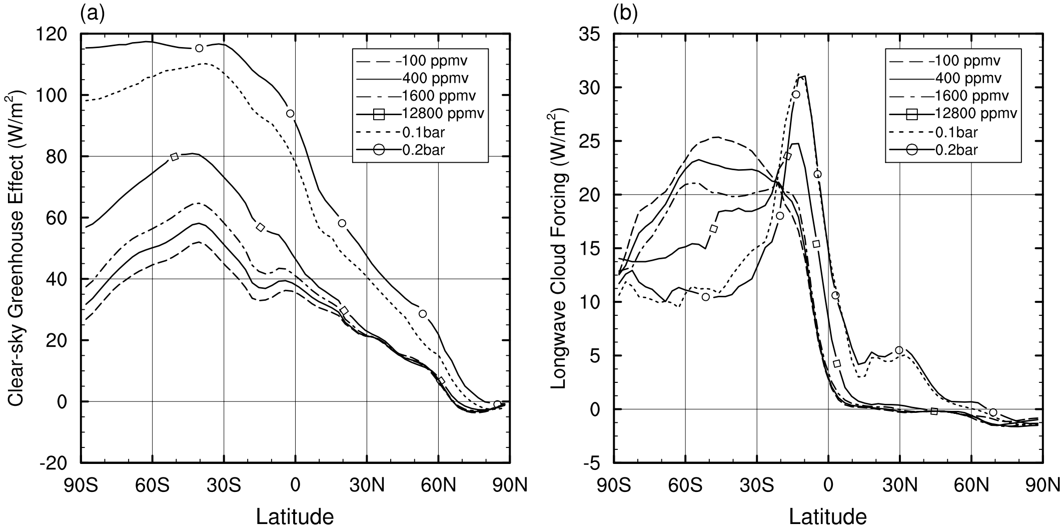

**Fig. 2.** January zonal-mean clear-sky greenhouse effect **(a)** and longwave cloud forcing **(b)** for various $CO_2$ levels.

CPD
6, 1337–1350, 2010

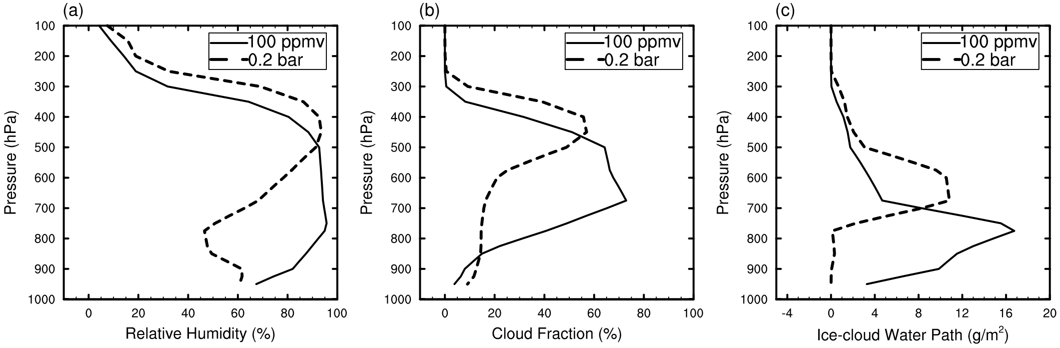

**Fig. 3.** Vertical distributions of relative humidity **(a)**, cloud fraction **(b)**, and ice-cloud water path **(c)**, averaged between 30° S and 60° S.

Title Page
Abstract
Introduction
Conclusions
References
Tables
Figures
|◀
▶|
◀
▶
Back
Close
Full Screen / Esc
Printer-friendly Version
Interactive Discussion

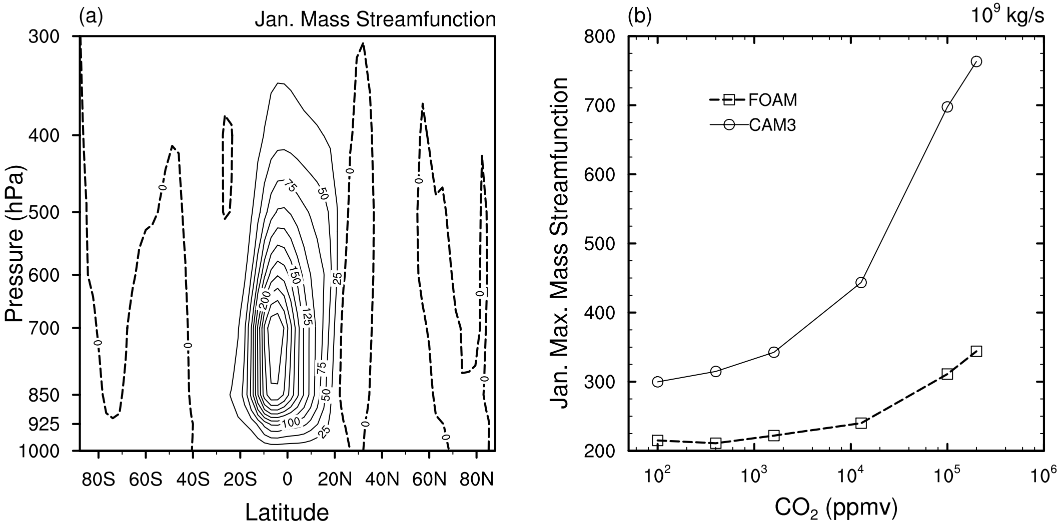

**Fig. 4.** **(a)** January meridional mass streamfunction for 100 ppmv of $CO_2$. Contour interval is $25 \times 10^9\ \mathrm{kg\,s^{-1}}$. **(b)** January maximum mass streamfunctions as a function of $CO_2$ level.

Title Page
Abstract
Introduction
Conclusions
References
Tables
Figures
◀▮ ▶▮
◀ ▶
Back
Close
Full Screen / Esc
Printer-friendly Version
Interactive Discussion